Aggregation Behavior of Halogenated Squaraine Dyes in Buffer, Electrolytes, Organized Media, and DNA

Kalliat T. Arun,[†] Bernd Epe,[‡] and Danaboyina Ramaiah*[,†]

Photochemistry Research Unit, Regional Research Laboratory (CSIR), Trivandrum 695 019, India, and Institute of Pharmacy, University of Mainz, D 55099 Mainz, Germany

Received: March 27, 2002; In Final Form: September 4, 2002

Aggregation properties of bis(3,5-dibromo-2,4,6-trihydroxyphenyl)squaraine (**1**) and bis(3,5-diiodo-2,4,6-trihydroxyphenyl)squaraine (**2**) have been examined in buffer and in the presence of electrolytes, β-cyclodextrin, micelles and DNA. These dyes were found to form aggregates in buffer and methanol−water solutions that have absorption bands blue-shifted to those of the monomeric forms. The iodo derivative **2** forms aggregates at much lower concentrations (1.7×10^{-6} M) compared to the bromo derivative **1** (2.35×10^{-6} M) in 20% (vol/vol) methanol−buffer solution. Increase in methanol concentration in methanol−water solutions resulted in the disruption of the aggregates. The intermediate dimer in the monomer to aggregate conversion process can be detected under specified conditions. The entropy and the standard free energy for the dimer formation in the case of **1** are found to be −16.12 eu and 7.46 k cal mol^{-1}, respectively. Addition of electrolytes (LiCl, NaCl, and KCl) and calf thymus DNA resulted in the enhancement of aggregate formation, whereas the monomer gets stabilized for several hours in the presence of microheterogeneous media such as β-cyclodextrin and cetyltrimethylammonium bromide. These results reveal that face-to-face stacking followed by hydrogen bonding interactions between the chromophoric units are the major driving force for the formation of sandwich (H-type) aggregates. These dyes exhibit favorable photophysical properties and can be applied into the tissues using carrier systems in which they do not form aggregates and hence can have potential use as sensitizers in photodynamic therapeutical applications.

Introduction

Photodynamic therapy (PDT) is emerging as a viable method for the treatment of cancer and it involves the inactivation of living cells by the combined action of visible light and a photosensitizer.[1−4] When injected into the body, the photosensitizer selectively accumulates in the tumor tissue. On irradiation with visible light, the sensitizer generates cytotoxic agents in the cell, which causes cell death and often tumor necrosis. PDT is relatively a safer treatment since the induction of cytotoxicity by PDT ceases when the light is switched off, contrary to the conventional chemotherapy and radiotherapy. Several photosensitizers have been investigated for their use in PDT. These include porphyrins, chlorins, benzoporphyrins, benzoporphycenes, phthalocyanins, purpurins, and aminolevulinic-acid-mediated porphyrins.[1−11] Among these, hematoporphyrin derivative (HpD) and its commercial variants have been approved for the treatment of various types of tumors in a number of countries.[12] However, these sensitizers have several disadvantages and hence the search for more effective sensitizers has become important in recent years.

Squaraines form a class of dyes possessing sharp and intense absorption in the near-infrared region.[13,14] Even though their photophysical and photochemical characteristics make them highly suitable for various industrial applications, their potential use as photosensitizers in PDT have not yet been explored. We have recently reported[15] that sensitizers based on squaraine moiety, such as bis(3,5-dibromo-2,4,6-trihydroxyphenyl)-squaraine (**1**) and bis(3,5-diiodo-2,4,6-trihydroxy- phenyl)-squaraine (**2**), can have potential use in PDT (Figure 1). Substitution with heavy atoms, such as bromine and iodine, in these systems resulted in increased water solubility and intersystem crossing efficiency, when compared to the unsubstituted squaraine dye. The singly deprotonated forms of **1** and **2** which are expected to be present predominantly under the physiological pH conditions exhibited significant triplet quantum yields ($\Phi_T = 0.5$ for **2**) and interact with molecular oxygen generating singlet oxygen ($\Phi(^1O_2) = 0.47$ for **2**) in quantitative yields.[15]

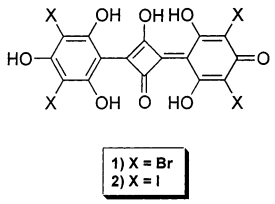

Figure 1. Structures of the halogenated squaraine dyes, under investigation.

Squaraine dyes are known to form aggregates in solutions,[16,17] organized media,[18,19] Langmuir−Blodget films,[18,20] and in microcrystals.[21] Depending on the nature of substituents and the medium, these dyes are found to form H-aggregates, in which each molecule is placed one above the other as a card pack, as well as J-aggregates, where each molecule is arranged in a head to tail fashion.[16−23] The aggregate formation significantly alters the photochemical properties of dyes including the generation of cytotoxic agents[24] and hence can play a significant role in PDT applications.

* To whom correspondence should be addressed. Photochemistry Research Unit, Regional Research Laboratory (CSIR), Trivandrum 695 019, India. Tel: +91 471 515321. Fax: +91 471 490186. E-mail: d_ramaiah@rediffmail.com or rama@csrrltrd.ren.nic.in.

[†] Photochemistry Research Unit.

[‡] Institute of Pharmacy.

10.1021/jp020816h CCC: $22.00
Published on Web 10/15/2002

In our efforts to evaluate the use of halogenated squaraine dyes **1** and **2** as sensitizers in PDT applications, we have examined their photophysical properties in buffer and in the presence of electrolytes, organized media, and DNA. Results of these studies reveal that **1** and **2** form aggregates in water−methanol mixture at higher concentrations and the aggregation process in these dyes was enhanced by the addition of electrolytes and calf thymus DNA. On the other hand, the presence of drug carriers, such as β-cyclodextrin, and membrane models, such as cetyltrimethylammonium bromide, stabilize the monomers of **1** and **2** for several hours indicating the potential use of these dyes as sensitizers in PDT applications.

Experimental Section

General Aspects. The equipment and procedures for melting point determination and spectral recording are described in earlier papers.[25,26] Calf thymus DNA concentration was determined as reported in the literature (ϵ, 6600 M^{-1} cm^{-1} at 260 nm).[27,28] An Elico pH meter was used for pH measurements. NaOH, NH_4OH or HCl were used to vary the pH of the solutions. Phosphate buffer (pH 6.4 and 7.4) used was contained KH_2PO_4 (10 mM) and NaCl (50 mM). Solutions for optical measurements were prepared from freshly prepared stock solution of the dye in methanol. Solvents used were purified before use. Doubly distilled water was used in all the studies. All experiments were carried out at room temperature (25 ± 1 °C), unless otherwise mentioned.

Chemicals. Calf thymus DNA (CT DNA), cetyltrimethylammonium bromide (CTAB) and β-cyclodextrin (β-CD) (all from Aldrich) were used without further purification. Squaric acid was a gift from Professor W. Adam, University of Wurzburg, Germany. The synthesis of bis(3,5-dibromo-2,4,6-trihydroxyphenyl)squaraine (**1**) and bis(3,5-diiodo-2,4,6-trihydroxyphenyl)squaraine (**2**) has been described elsewhere.[15]

Absorption and Fluorescence Measurements. Absorption and emission spectra were recorded on Shimadzu UV-3101 PC NIR scanning spectrophotometer and SPEX-Fluorolog F112X spectrofluorimeter, respectively. The concentration dependence studies were carried out by adding the dye solution in methanol to water or buffer and allowing it to stand for 15 min before recording the spectra. Since the aggregate formation was time dependent, the effect of electrolytes and organized media was examined by adding the dye solution in methanol to the already made solutions of the electrolytes or organized media and recording the spectra immediately after addition. Buffer (pH 6.4) was used in all experiments so that only the singly deprotonated form of squaraine dyes **1** and **2** exist in the solution. Thermodynamic parameters were determined in 2% (vol/vol) methanol−water mixture for convenience. All experiments were carried out at least twice with consistent results.

Results and Discussion

Characterization of Dye Aggregates. The absorption spectra of squaraine dye **1** in 20% (vol/vol) methanol−buffer mixture, recorded at different concentrations are shown in Figure 2. At lower concentrations (<2.35×10^{-6} M), the dye exhibits a sharp absorption at 610 nm with a weak shoulder, but at higher concentrations, a new broad band centered around 560 nm appears. Addition of methanol to this solution resulted in the decrease in absorbance at 560 nm with the concomitant increase in absorption at 610 nm. This confirms the fact that the absorption at 560 nm is not due to any of the four species in which the dye is known to exist,[15] but due to the association between the individual dye molecules (aggregates). Since on adding methanol, the absorbance at 610 nm increases with the decrease in absorbance at 560 nm, we presume that face-to-face stacking of the monomers followed by intermolecular hydrogen bonding interactions are the driving force behind the aggregate formation. In the case of the iodo derivative **2**, the aggregate formation was observed at much lower concentrations (1.7×10^{-6} M) presumably due to the presence of larger iodine atoms.

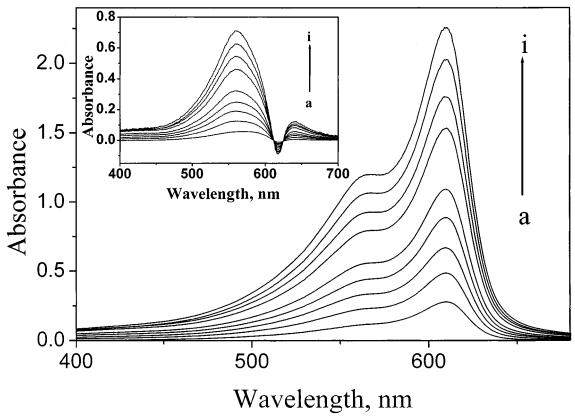

Figure 2. Absorption spectra of **1** at different concentrations in 20% (vol/vol) methanol−buffer (pH 6.4) mixtures. [**1**] (a) 2.42×10^{-6} M, (i) 24.2×10^{-6} M. Inset shows the deconvoluted spectra of the aggregates obtained by subtracting the monomer spectra from the combined spectra of monomer and aggregate.

The role of hydrogen bonding in the aggregation of these dyes was investigated by studying the aggregation phenomenon in various proportions of methanol−buffer mixture. Figure 3 shows the change in absorbance with increase in concentration of **1** in different methanol−buffer mixtures. In 2% (vol/vol) methanol−buffer mixture (Figure 3A), the peak around 560 nm appears even at very low concentration of the dye (0.72×10^{-6} M). This peak increases as the concentration of the dye in the solution increases. Similar observation was made in 10% (vol/vol) methanol−buffer mixture (Figure 3B), but the aggregate was formed only at a higher concentration (2.4×10^{-6} M) of the dye. In the case of 30% (vol/vol) methanol−buffer mixture (Figure 3C), no peak around 560 nm was observed even at very high dye concentrations. This reveals that practically no aggregate is formed at this proportion of methanol and buffer thereby proving the role of hydrogen bonding interactions in the aggregate formation.

Another interesting observation made was the tendency of these dyes to form higher order aggregates. Inset of Figure 3B shows the plot of log[monomer] versus log[aggregate] for **1** in 10% (vol/vol) methanol−buffer mixture. As can be seen from the Figure, the plot was found to be nonlinear with the increase in concentration of the dye. This clearly indicates that **1** has a tendency to form higher order aggregates as the concentration of the dye increased in methanol−buffer mixtures.

Since there is considerable spectral overlap between the monomer and aggregate at the peak positions, the concentrations of the monomer and aggregate could not be estimated from the observed spectrum. Therefore, the concentration of these species was estimated by spectral deconvolution method. The normalized monomer spectrum (obtained at very low dye concentration) was subtracted from the spectrum that contained both the monomer and aggregate absorption (inset of Figure 2) thereby the concentration of the aggregate and monomer was estimated. A plot of log [monomer] versus log [dimer] gave a straight line (Figure 4) with a slope of 2 indicating thereby that the aggregate is a dimer.

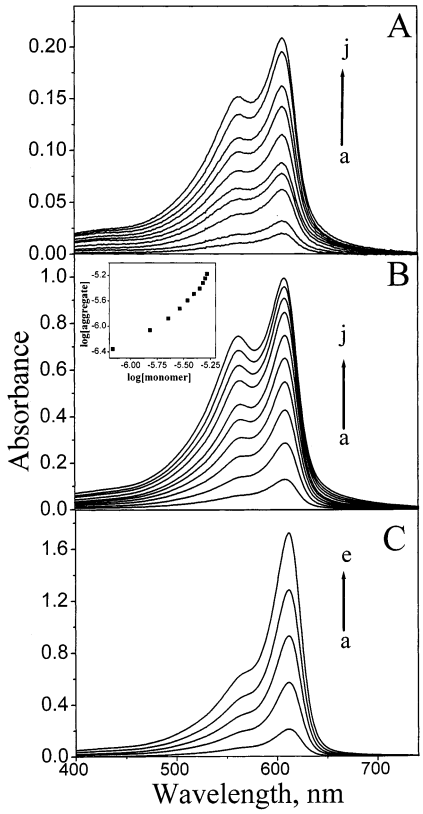

Figure 3. Absorption spectra of **1** at different concentrations in (A) 2%, (B) 10%, and (C) 30%, (vol/vol) methanol−buffer (pH 6.4) mixtures. Figure A: [**1**] (a) 0.24×10^{-6} M, (j) 2.39×10^{-6} M. Figure B: [**1**] (a) 1.12×10^{-6} M, (j) 1.19×10^{-5} M. Figure C: [**1**] (a) 1.19×10^{-6} M, (e) 1.19×10^{-5} M. Inset of Figure B shows the plot of log[monomer] versus log[dimer] for solutions of **1** in 10% (vol/vol) methanol−buffer (pH 6.4) mixtures.

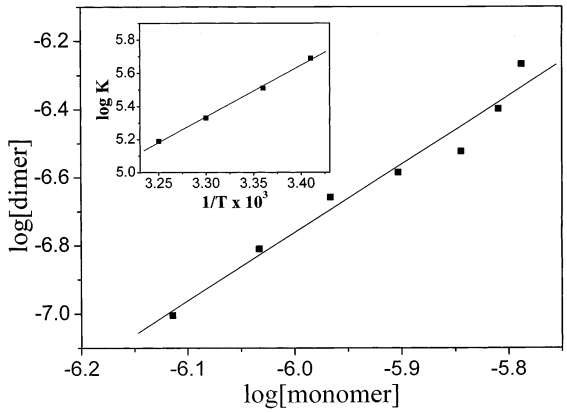

Figure 4. Plot of log[monomer] versus log[dimer] for solutions of **1** in 2% (vol/vol) methanol−water mixture. Inset shows the Arrhenius plot of log K versus $1/T$ for **1**.

To have a better understanding of the dimer formation, we determined the thermodynamic functions of this association process. Enthalpy of the dimer formation (ΔH) has been calculated using the Van't Hoff equation and the aggregation constant at different temperatures (Table 1). The Arrhenius plot of log K versus $1/T$ is shown as an inset of Figure 4. The standard free energy (ΔG) and entropy change (ΔS) have been calculated using the eqs 1 and 2, and are

$$\Delta G = -RT \ln K \quad (1)$$

$$\Delta S = (\Delta H - \Delta G)/T \quad (2)$$

found to be 7.46 kcal mol^{-1} and −16.12 eu, respectively.

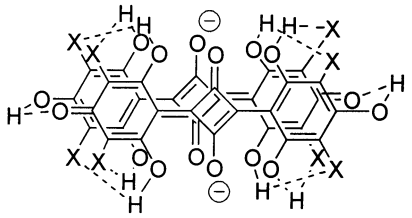

Figure 5. Schematic representation of dimer (H-aggregate) formed from **1** and **2.**

TABLE 1: Equilibrium Constant (K) and Thermodynamic Functions for the Dimerization of 1 in 2% (vol/vol) Methanol−Water Mixture

temp, K	K, 10^5 M^{-1}	$-\Delta G$, kcal mol^{-1}	$-\Delta H$, kcal mol^{-1}	ΔS, eu
293	6.21	7.46	8.08	−16.12
298	3.71			
303	1.97			
305	1.42			

Various interactions, such as hydrogen bonding, hydrophobic and van der Waal's interactions, can lead to aggregation. In the presence of electrolytes, coordination of the dye with ions can also result in aggregation. Depending on the structure of the molecule, one of these mechanisms predominates in the formation of the dye aggregates. Figure 5 shows the H-aggregate formed by the association of the dye molecules in which one molecule is arranged over the other. The proposed face-to-face geometry is also suitable for the formation of intermolecular hydrogen bonding interactions between electronegative halogen atoms of the one squaraine and the hydroxyl groups of the another as shown in Figure 5. The two squaraine moieties have to be antiparallel to each other so that the extent of hydrogen bonding would be maximum. Since we observe the formation of higher order aggregates in 10% (vol/vol) methanol−buffer mixtures, hydrophobic, and van der Waal's interactions between the dye molecules also contribute to the aggregate formation under these conditions.

Effect of Electrolytes on Aggregation. The addition of the electrolyte to the dye solutions has been observed to cause changes in the extent of dye aggregation, or what is known as the salt effect.[23,29,30] There are also reports in the literature[31,32] where the addition of electrolytes was found to quench the fluorescence of the dye and enhance the formation of aggregate by a factor of 2. To find out how the electrolytes affect the aggregate formation, we investigated the absorption and fluorescence emission properties of the squaraine dyes **1** and **2** in the presence of electrolytes, such as LiCl, NaCl, and KCl. Figure 6 shows the effect of LiCl on the absorption spectra of **1** in 20% (vol/vol) methanol−water mixtures. It is clear from the Figure 6 that addition of LiCl to a solution of the dye resulted in a decrease in the monomer absorbance at 610 nm with an enhancement in aggregate absorbance at 560 nm. Addition of NaCl and KCl also yielded similar results. Among the three electrolytes examined, LiCl induced the maximum effect. Similar observations were made in the case of the iodo derivative **2**.

After electrolytes were added to a solution of the dye **1**, quenching of the fluorescence was observed (inset of Figure 6). A blue shift in the emission maximum from 630 to 623 nm was observed along with the quenching of the fluorescence emission. Plotting the change in fluorescence emission against the electrolyte concentration, we compared the extent of decrease in fluorescence emission induced by the three electrolytes. Figure 7 shows the Stern−Volmer plots for the quenching of fluorescence emission of **1** by various salts. The Stern−Volmer

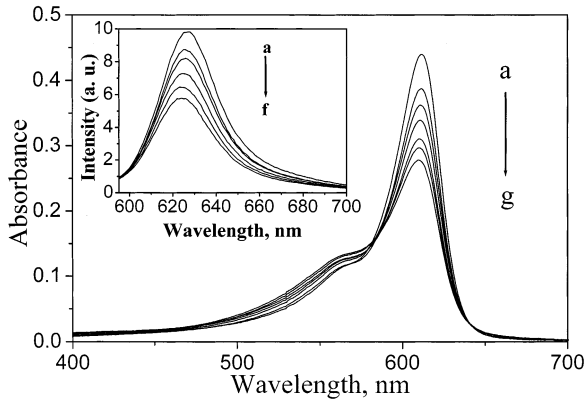

Figure 6. Effect of LiCl on the absorption spectra of **1** (2.3×10^{-6} M) in 20% (vol/vol) methanol−water mixture. [LiCl] (a) 0 M, (g) 0.18 M. Inset shows the effect of LiCl on the emission spectra of **1** in 20% (vol/vol) methanol−water mixtures. [LiCl] (a) 0 M, (f) 0.18 M. Excitation wavelength 575 nm.

quenching constant (K_{sv}) was determined by using eq 3,

$$I_0/I = 1 + K_{SV}[Q] \tag{3}$$

where I_0 and I are the fluorescence intensities in the absence and presence of the quencher, K_{SV} is the Stern−Volmer constant, and [Q] is the quencher concentration. It was found that the Stern−Volmer quenching constant for **1** by LiCl was 3 and 14 times higher than that for NaCl and KCl, respectively. The quenching of fluorescence can be attributed to the formation of aggregates, and confirms the fact that the aggregate is formed from the singly deprotonated form of the dye.

The efficient fluorescence quenching of squaraine dyes by the electrolytes confirms the fact that these dyes exhibit specific complexation with the positive ions and results in the aggregate formation. Of the positive ions examined, Li^+ induced the maximum effect. Lithium being the small ion, it is easily hydrated thereby empties the water molecules present between the monomer units. Furthermore, its positive charge density can efficiently polarize the electronic cloud present on the anionic species of the dye, thereby reducing the electron repulsion between the monomers. Therefore, we observed a significant enhancement in aggregation of these dyes in the presence of LiCl and a decrease in K_{sv} in the order $Li^+ > Na^+ > K^+$.

Considering the thermodynamic stability of the aggregation, the following eqs 4−6 can be proposed for the formation of aggregates of **1** and **2** in the

$$Sq + M \overset{K_1}{\rightleftharpoons} SqM \tag{4}$$

$$SqM + Sq \overset{K_2}{\rightleftharpoons} Sq_2M \tag{5}$$

$$K = K_1K_2 = [Sq_2M]/[Sq]^2[M] \tag{6}$$

presence of electrolytes,[29] where Sq and M are the concentrations of the squaraine dye and electrolyte, respectively, and K is the association constant. On the bases of these equations, the association constant K for the complexes formed between the squaraine dyes and various metal ions was calculated and are found to increase in the order KCl < NaCl < LiCl for both **1** and **2**. In the case of **2**, a constant value of $K = 1.3 \times 10^6$ was observed for LiCl at the concentrations studied, showing the formation of a dimer, whereas in the case of NaCl and KCl, the constant value for K was obtained only at higher concentrations. These results suggest that both the complexation reactions

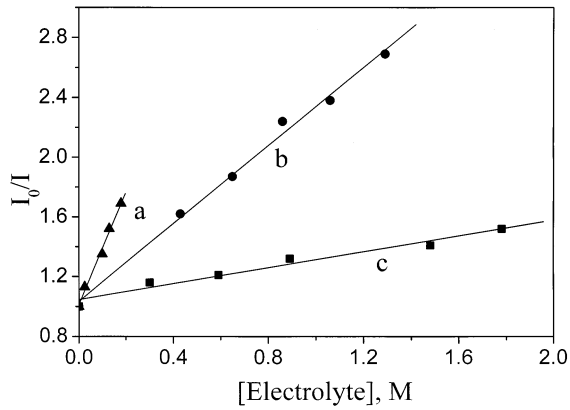

Figure 7. Stern−Völmer plot for the quenching of fluorescence of **1** (3.0×10^{-6} M) by electrolytes. (a) LiCl, (b) NaCl, (c) KCl.

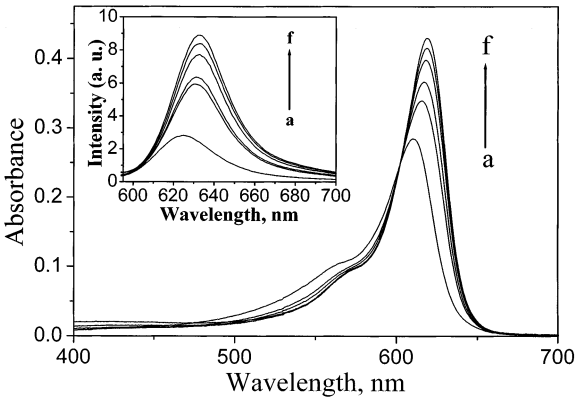

Figure 8. Effect of β-CD on the absorption spectra of **1** (1.6×10^{-6} M) in 20% (vol/vol) methanol−buffer (pH 6.4) mixture. [β-CD] (a) 0 M, (f) 3.4×10^{-3} M. Inset shows the effect of β-CD on the emission spectra of **1**. [β-CD] (a) 0 M, (f) 3.4×10^{-3} M. Excitation wavelength 575 nm.

as well as electrostatic screening effects of electrolytes control the formation and stability of the aggregates of **1** and **2**.

Effect of β-CD, CTAB, and DNA. To have a fair idea about how various organized media affect the aggregation, the absorption and emission properties of squaraine dyes **1** and **2** were examined in the presence of drug carrier systems such as β-cyclodextrin (β-CD), membrane mimics, such as cetyltrimethylammonium bromide (CTAB), and biopolymers, such as calf thymus DNA (CT DNA). It is well-known that β-CD forms inclusion complex[33] with the guest molecules and CTAB forms micellar structure thereby providing in them both the hydrophobic and hydrophilic environment.[34]

Figure 8 shows the effect of β-CD on the absorption spectra of **1** in 20% (vol/vol) methanol−buffer solutions. Addition of **1** to the buffer solution containing β-CD resulted in the enhancement of the monomer absorbance with a bathochromic shift of 8 nm. The enhancement reached saturation at 3.4×10^{-3} M of β-CD. The fluorescence emission of these dyes was also enhanced in the presence of β-CD (inset of Figure 8) with a bathochromic shift of about 8 nm. We did not observe any new peak around 560 nm in the absorption spectra of the dye in the presence of β-CD. This indicates that in the presence of β-CD, the squaraine dye does not aggregate even in buffer solutions. Similar results were obtained with CTAB, however; the saturation was observed at 19×10^{-3} M of CTAB. In contrast, CT DNA was found to enhance the aggregation of both the squaraine dyes **1** and **2** as monitored by the absorption and fluorescence spectroscopy (see Supporting Information,

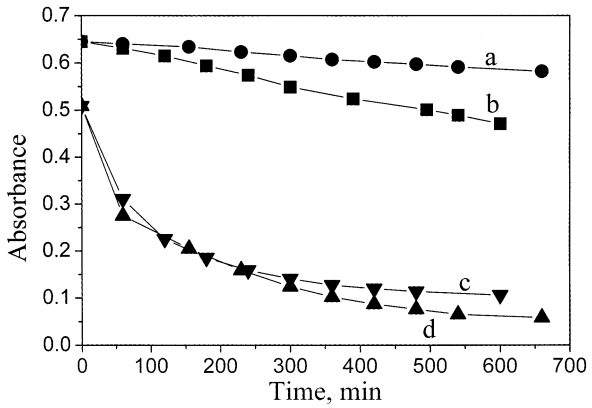

Figure 9. A plot of absorbance of **1** (3.0×10^{-6} M) vs time in 20% (vol/vol) methanol−buffer (pH 6.4) mixture. (a) [CTAB] 10×10^{-3} M, (b) [β-CD] 3.2×10^{-3} M, (c) [CT DNA] 2.44×10^{-3} M, and (d) dye **1** alone.

Figure 12S). DNA acts similar to the electrolytes in inducing the aggregation of these dyes.

The bathochromic shifts in the absorption and fluorescence properties in the presence of β-CD can be attributed to the formation of inclusion complexes between β-CD and squaraine dyes **1** and **2**. Benesi-Hildebrand analysis[35] of the change in fluorescence emission of these dyes with β-CD concentration indicated the formation of a 2:1 complex between β-CD and squaraine dyes. Due to this complex formation, the monomeric species gets encapsulated inside the β-CD cavity thereby being unable to form aggregates. The enhancement of fluorescence in the presence of β-CD can be attributed to the decrease in rotational freedom of the encapsulated molecule and elimination of the quencher water molecules from the immediate surroundings. Similarly, the microencapsulation of the dyes **1** and **2** in the presence of CTAB results in the inhibition of aggregate formation.

To find out whether aggregate formation is completely prevented in the presence of the organized media, we have monitored the change in absorbance of the monomer with time. Figure 9 shows the change in absorbance of the dye **1** with time in the presence of β-CD, CTAB, and CT DNA. In the presence of CT DNA and absence of organized media, decrease in the monomer absorbance with time was observed with the increase in formation of the dye aggregates. However, in the presence of organized media (β-CD and CTAB), the decrease in the absorption of the monomer was very marginal. Of these, CTAB was found to stabilize the monomer to a greater extent than β-CD. The aggregation of these dyes was not completely prevented in the presence of the organized media but the stabilization of the monomer could be extended to several hours (Figure 9) when compared to the changes observed in buffer. These results reveal that the stabilization of the active forms of **1** and **2** can be achieved in the presence of the organized media and hence reflects their potential use as sensitizers in PDT applications where the drug can be delivered at the required point using various carrier systems.

Conclusion

In summary, the results obtained in this study confirm that squaraine dyes **1** and **2** form aggregates in methanol−buffer solutions at higher concentrations and the aggregates formed are of H-type. The face-to-face geometry of the H-aggregate is also suitable for the intermolecular hydrogen bonding interactions between the electronegative atoms of the one squaraine unit and the hydroxyl groups of the another, which renders stability to the aggregate. The iodo derivative **2** forms aggregate at much lower concentrations than the bromo derivative **1**. Electrolytes such as LiCl, NaCl, KCl, and biopolymer such as CT DNA enhanced the aggregate formation, whereas the aggregation of these dyes could be prevented, to a large extent, by encapsulating them in carrier systems, such as β-CD, and membrane mimics, such as CTAB. These results demonstrate that the squaraine dyes **1** and **2** can have potential use as sensitizers in the photodynamic therapy of cancer where they can be administered into the body using carrier systems, such as liposomes, which prevent their aggregation inside the body.

Acknowledgment. The authors thank the Council of Scientific and Industrial Research, Government of India and the Volkswagen Foundation, Germany, for the financial support of this work and Mahesh Hariharan for helpful suggestions. This work represents document RRLT-PRU-136 from the Photochemistry Research Unit, Regional Research Laboratory.

Supporting Information Available: Absorption spectra of **1** and **2** at various concentrations in 2% (vol/vol) methanol−water mixture, absorption and emission spectra of **1** in the presence of NaCl, KCl, CTAB, and CT DNA; absorption and emission spectra of **2** in the presence of LiCl, NaCl, KCl, β-CD, and CTAB; and the Stern-Völmer plot for the quenching of fluorescence of **2** by electrolytes. This material is available free of charge via the Internet at http://pubs.acs.org.

References and Notes

(1) Dougherty, T. J. *Photochem. Photobiol*. **1987**, *45*, 879.
(2) Bonnett, R. *Chem. Soc. Rev*. **1995**, *24*, 19.
(3) MacRobert, A. J.; Philips, D. *Chem. Ind*. **1992**, 17.
(4) Kessel, D. *Photodynamic Therapy of Neoplastic Disease*; CRC Press: Boca Raton, FL, 1990; Vol. 2.
(5) Moan, J.; Berg, K. *Photochem. Photobiol*. **1992**, *55*, 931.
(6) Gomer, C. J. *Photochem. Photobiol.* **1991**, *54*, 1093.
(7) Brown, S. B.; Truscott, T. G. *Chem. Br*. **1993**, *29*, 955.
(8) Fiery P. A.; Ford, W. E.; Sounik, J. R.; Kenney, M. E.; Rodgers, M. A. J. *J. Am. Chem. Soc.* **1988**, *110*, 7626.
(9) Jori, G.; Spikes, D. In *Topics in Photomedicine*; Smith, K. C. Ed.; Plenum Publishing Corp.: New York, 1984; p 183.
(10) Garbo, G. M. *J. Photochem. Photobiol., B.* **1996**, *34*, 109.
(11) Moser, J. G. *Photodynamic Tumor Therapy: 2nd and 3rd Generation Photosensitizers*; Harwood Academic Publishers: Amsterdam, 1998.
(12) Levy, J. G. *Trends Biotechnol*. **1995**, *13*, 14.
(13) Law, K. Y. *J. Phys. Chem.* **1987**, *91*, 5184.
(14) Law, K. Y. *J. Phys. Chem.* **1995**, *99*, 9818.
(15) Ramaiah, D.; Joy, A.; Chandrasekhar, N.; Eldho, N. V.; Das, S.; George, M. V. *Photochem. Photobiol*. **1997**, *65*, 783.
(16) Buncel, E.; McKerrow, A.; Kazmaier, P. M. *J. Chem. Soc., Chem. Commun*. **1992**, *17*, 1242.
(17) Das, S.; Thanulingam, T. L.; Thomas, K. G.; Kamat, P. V.; George, M. V. *J. Phys. Chem*. **1993**, *97*, 13620.
(18) Chen, H.; Herstroeter, W. G.; Perlstein, J.; Law, K. Y.; Whitten, D. G. *J. Phys. Chem.* **1994**, *98*, 5138.
(19) Das, S.; Thomas, K. G.; Thomas, K. J.; Madhavan, V.; Liu, D.; Kamat, P. V.; George, M. V. *J. Phys. Chem.* **1996**, *100*, 17310.
(20) Law K. Y.; Chen, C. *J. Phys. Chem*. **1989**, *93*, 2533.
(21) Law K. Y. *J. Phys. Chem*. **1988**, *92*, 4226.
(22) McRae, E. G.; Kasha, M. In *Physical processes in Radiation Biology*; Augenstein, L., Rosenberg, B., Mason, S. F., Eds.; Academic Press: New York, 1963; pp 23−42.
(23) Chen, H.; Farahat, M. S.; Law, K. Y.; Whitten, D. G.; *J. Am. Chem. Soc*. **1996**, *118*, 2584.
(24) Aveline, B. M.; Hasan, T.; Redmond, R. W. *J. Photochem. Photobiol., B. Biol*. **1995**, *30*, 161.
(25) Sajimon, M. C.; Ramaiah, D.; Thomas, K. G.; George, M. V. *J. Org. Chem*. **2001**, *66*, 3182.
(26) Ramaiah, D.; Muneer, M.; Gopidas, K. R.; Das, P. K.; Rath, N. P.; George, M. V. *J. Org. Chem.* **1996**, *61*, 4240.
(27) Chen. Y.-H.; Lown, J. W. *J. Am. Chem. Soc*. **1994**, *116*, 6995.
(28) Adam, W.; Cadet, J.; Dall′Acqua, F.; Epe, B.; Ramaiah, D.; Saha-Möller, C. R. *Angew. Chem., Int. Ed. Engl.* **1995**, *34*, 107.

(29) Valdes-Aguilera, O.; Neckers, D. C. *Acc. Chem. Res.* **1989**, *22*, 171.
(30) Burdett, B. C. *Aggregation Processes in Solution*; Wyn-Jones, E.; Gormally, J. Eds.; Elsevier: New York, 1983; pp 241−242.
(31) Isak, S. J.; Eyring, E. M. *J. Phys. Chem.* **1992**, *96*, 1738.
(32) Nuesch, F.; Grätzel, M. *Chem. Phys.* **1995**, *193*, 1.
(33) Ueno, A.; Osa, T. In *Photochemistry in Organized and Constrained Media*; Ramamurthy, V., Ed.; VCH Publishers: New York, 1991; pp 739−782.
(34) Kalyanasundaram, K. *Photochemistry in Microheterogeneous Systems*; Academic Press: New York, 1987.
(35) Benesi, H. A.; Hildebrand, J. H. *J. Am. Chem. Soc.* **1949**, *71*, 2703.